14 **IMPACT OF WIND SHEAR ON THE TOP OF STRATOCUMULUS CLOUD**

M. K. Kopeć[1]*, S. P. Malinowski[1], Z. P. Piotrowski[2]

[1] Institute of Geophysics, Faculty of Physics, University of Warsaw, Warsaw, Poland

[2] Institute of Meteorology and Water Management - National Research Institute, Warsaw, Poland

1 INTRODUCTION

Analyzing data from Physics of Stratocumulus Top (POST) campaign (Gerber et al., 2013) two different types of stratocumulus were revealed (Malinowski et al., 2013):

- "classical", under strong temperature inversion, dry air above the cloud top and thin wind shear layer in the cloud top region;
- "non-classical" under weak temperature inversion, humid air above and deep shear layer.

More detailed analysis indicated that mixing at the top of "classical" stratocumulus may produce negative buoyancy, i.e. it allows for Cloud Top Entrainment Instability (CTEI), while "non-classical" cases prohibit CTEI.

Since typical Large Eddy Simulations (LES) simulations of stratocumulus clouds are based on "classical" experimental or idealized cases (see e.g. Stevens et al., 2005, and references therein), a representative of "non-classical" cases (TO13) was chosen for numerical examination. Namely, series of LES were performed in order to investigate such type of Sc. The goal was to compare simulated cloud with in-situ data and to analyze in detail dynamics and mixing on the top of "non-classical" cloud.

2 LARGE EDDY SIMULATION

As the numerical framework we used the recently developed version of EULAG model (Prusa et al., 2008, Piotrowski et al., 2011) with three-dimensional MPI decomposition. Vertical domain decomposition improves performance by improving memory locality and minimizing communicated halo size, especially pronounced for grids with large number of points in the vertical (Piotrowski et al., 2011). Since the experimental results suggest presence of multiple thin sub-layers in the proximity of cloud top, anisotropic grid with refined vertical resolution of 20 x 20 x 2.5 m was used. Similar aspect ratio but lower resolution was already used in EULAG simulations by (Kurowski et al., 2009). Horizontally periodic domain extending 4 x 4 x 1.2 km was employed, with the time step of 0.3 s.

We focused on the effects of wind shear and radiative cooling on the details of cloud top structure and entrainment/mixing across capping inversion. Thus, the following simulations are analyzed:

- "ref" with no wind shear and no radiative cooling at the cloud top;
- "sh" with a shear layer across the cloud top and no radiative cooling;
- "rc" with radiative cooling and no shear;
- "shrc" including both: shear and radiative cooling effects.

2.1 Initial profiles and surface fluxes

Idealized profiles of potential temperature (left panel in Figure 1), horizontal wind vector components (middle panel), water vapor mixing ratio (right panel) and cloud water mixing ratio (dashed red lines in Figure 4) were constructed based on the airplane soundings taken in the course of TO13 research flight. Moreover, wind profile was prepared in two versions: first with the wind shear at the cloud top as was observed in the course of the flight, and the modified profile with no shear (dashed blue line in Figure 1).

Sensible and latent heat fluxes at the surface were constant throughout the simulation and equal to 5 W/m^2 and 10 W/m^2, respectively.

2.2 Mixing diagram

Notable feature of TO13 flight (see Gerber et al., 2013) was that the thermodynamic conditions prevented CTEI. Gerber et al. (2013) and Gerber et al. (2014) argue that the negative buoyancy, observed sometimes in "cloud holes" - regions of depleted LWC (liquid water content), was a result of radiative cooling. In order to test this hypothesis, idealized profiles of the temperature and humidity used in the simulations ensured that the buoyancy of mixed parcels is

*Corresponding author: Pasteura 7, 02–093 Warsaw, Poland, e–mail: mtrzask@igf.fuw.edu.pl

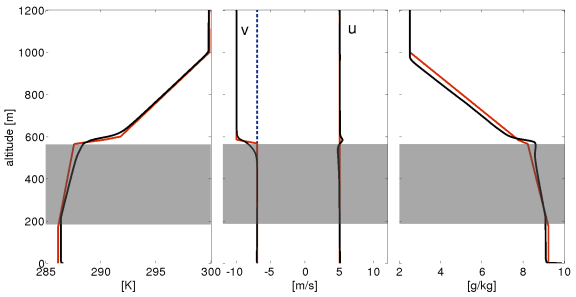

Figure 1: Initial profiles (red lined) and domain averaged profiles after 200 minutes of simulation (black lines). Dashed blue line in central panel marks initial wind profile for no shear cases. Grey boxes indicate region with cloud water. Left panel shows potential temperature, middle panel - horizontal wind components, right panel - water vapor mixing ratio.

the same as the buoyancy of cloud top, regardless of mixing proportions. Figure 2 presents the mixing diagram of the air from the cloud top and from above the inversion.

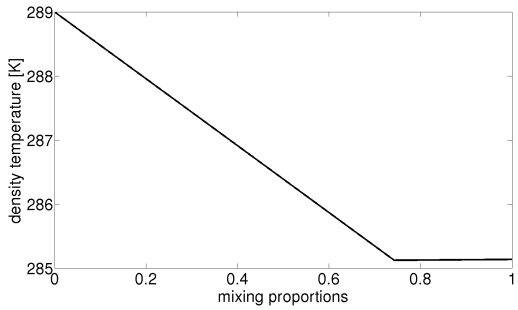

Figure 2: Mixing diagram. Mixing proportion equal to 0 means that no cloud top air was mixed with air from above the inversion, 1 - only cloud air was mixed.

2.3 Radiative cooling

In order to analyze the effects of radiative cooling, we introduced (following Stevens et al., 2005) a simple parameterization of long-wave radiative cooling, and tuned the parameters to match long-wave fluxes observed in the course of TO13 flight. As this was the afternoon flight, we neglected the effects of solar radiation.

Figure 3 presents the profile of long-wave radiation measured during TO13 (black line) and the idealized profile used in simulations, calculated with the equation 1:

$$F_{rad} = \begin{cases} F_0 e^{-\int_z^\infty k q_c dz} & z < z_i \\ F_0 e^{-\int_z^\infty k q_c dz} + C(z - z_i)^{1/2} & z \geq z_i \end{cases} \quad (1)$$

where, q_c - profile of liquid water mixing ratio in g/kg and z - altitude [m]. Parameter values used to calculate F_{rad} were: $F_0 = 80$ W m^{-2}, $k = 0.8$ m^{-1}, $C = 0.5$ W m$^{-5/2}$ and $z_i = 560$ m.

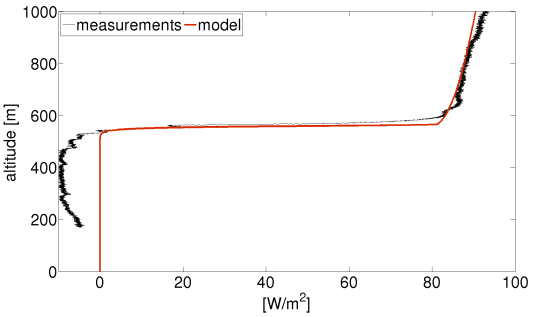

Figure 3: Profile of long-wave radiative flux measured during TO13 flight (black line) and calculated with equation 1 (red line).

In simulations "rc" and "shrc" the parameterization of radiative cooling was turned on after the spin-up period of the model (1.5 h simulated time). This was done in order to avoid the effect of radiative cooling on static, non-turbulent idealized initial cloud. The simulations were further continued up to 4 h of simulated time.

3 SIMULATED CLOUD

The following cloud properties were compared: profiles of liquid water mixing ratio at the end of simulations (left panel in Figure 4), time series of cloud top altitude (Figure 5) and time series of liquid water path (Figure 6). Domain averaged values are shown as lines, while variability is marked with gray shades.

3.1 Liquid water mixing ratio profiles

Figure 4 presents final profiles of liquid water mixing ratio (q_c) for all simulations. It can be seen that the differences in q_c are visible in the uppermost 120 m of the cloud. Unsurprisingly, the shear dilutes the cloud top, while radiative cooling increases q_c in cloud top region. Cautious inspections of profiles variability indicates that the effect of shear on the maximum altitude of cloudy blobs depends on the radiative cooling: decrease for "sh" simulation and increase for "shrc".

3.2 Cloud top altitude

The following Figure 5 shows the evolution of domain averaged cloud top height in the course of simulations. It can be seen, that cloud top height reacts to change in radiative cooling with the about 1.5 hour

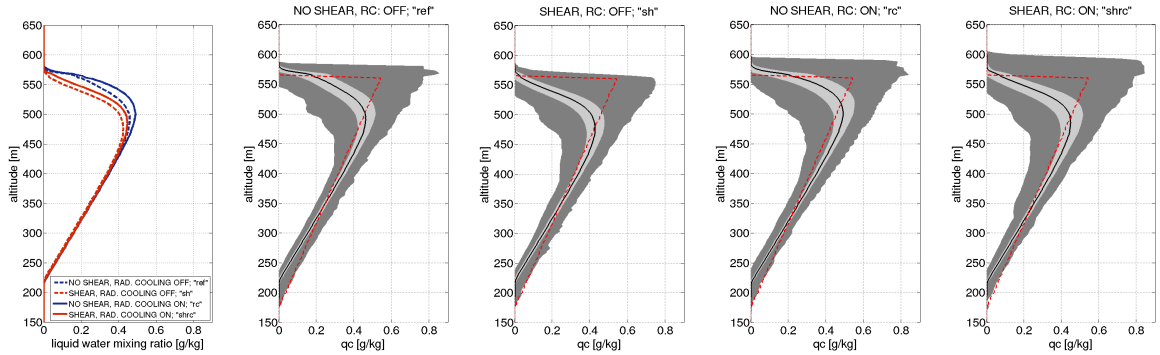

Figure 4: The left panel shows averaged profiles of liquid water mixing ratio (blue lines - simulations without wind shear, red lines - with shear, dashed lines - radiative cooling off, solid lines - radiative cooling on). In the other panels dark grey shading spans the range between the maximum and the minimum value at any given altitude. The light shading spans between the mean value plus/minus one standard deviation. Black line marks the model domain averaged profile and dashed red line marks the initial profile.

delay. This is the time comparable to the spin-off time of the model, which suggests that in the investigated case cloud top height is to a large extent governed by the convective eddies spanning the whole boundary layer (BL) and the response to radiative cooling is due to its effect on convective circulations.

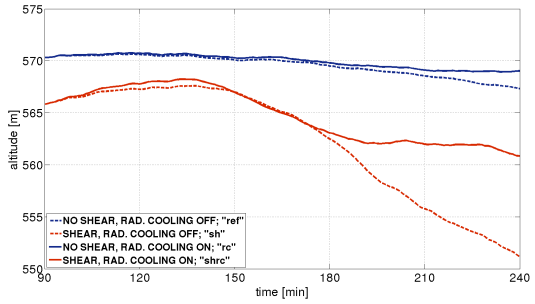

Figure 5: Color code as in left panel of figure 4.

After this delay cloud top height behaves in accordance with expectations: radiative cooling almost completely compensates cloud thinning from the top due to dilution by mixing.

3.3 Liquid water path

In contrary to the cloud top height, the liquid water path (LWP) reacts immediately to radiative cooling. In ”ref” simulation LWP stays almost constant during whole simulation. Turning on the radiative cooling (”rc” simulation) results in the increase of LWP values while presence of shear (”sh” simulation) starts to decrease it after 1.5 hour. Presence of both phenomena results in the increase of LWP in first 1.5 hour (after spin-up time) and later a stabilization.

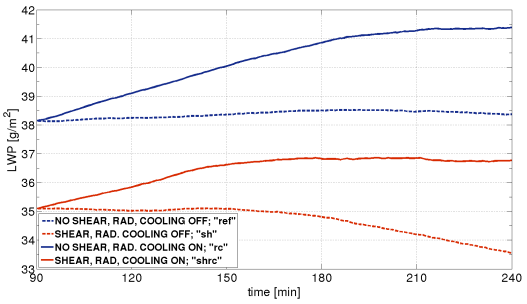

Figure 6: Color code as in left panel of figure 4.

4 VIRTIUAL AIRCRAFT

Virtual aircraft is a method to sample computational domain. The main goal of this method is to collect data in the virtual reality of the model in the same way as research aircraft performs measurements in a real cloud: along a prescribed trajectory and in the course of cloud evolution. For this exercise after spin-up time in "shrc" simulation several "virtual aircrafts" (a number increased to get a reasonable statistics) were sampling the computational domain along trajectories mimicking profiles and porpoises (consecutive ascents and descents in $\sim$200 m thick layer centered at the mean cloud top altitude) of the Twin Otter research aircraft in the coarse of real flight. For the comparison with domain averaged statistics data sampled in such a way from a 15 min period (200-215 min of simulation) were used. Results are shown in Figure 7.

The comparison indicates, that mean profiles of q_c and their standard deviations are adequately reproduced in virtual aircraft data. However, the tails of the distribution (extremal values) cannot be represented

in the much poorer statistics from the virtual aircraft. This suggests that this may be an issue with the real experimental data - their amount may be insufficient to produce fully adequate statistics.

In Figure 8 data collected by the virtual aircraft in the course of the simulation and by the real cloud in the course of the research flight are compared. The consecutive panels in left column present profiles from the porpoises of the virtual aircraft, corresponding panels in the right column presents data from TO13 flight. For this comparison measurements were averaged to the same time resolution as in the model.

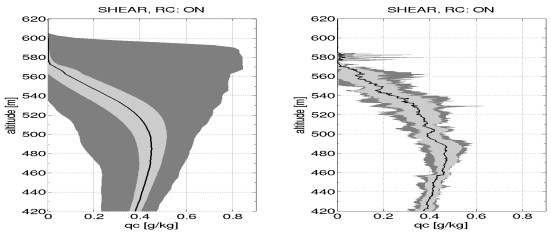

Figure 7: Comparison of virtual aircraft data statistics (right panel) with statistics from the whole model domain (left panel).

As one can see, character of data from real and virtual aircraft is the same. They however, differ substantially from vertical profiles along columns in the model domain (dashed black lines on left panels in Figure 8). This clearly indicates that fluctuations in airborne measurement taken along weakly inclined trajectories represent to a large extent horizontal variability of cloud properties.

5 CONCLUSIONS

- Wind shear dilutes the cloud (lower values of LWP and cloud top altitudes than in no shear cases; see Figures 5 and 6).
- In wind shear cases maximum value of q_c is smaller and is located on lower altitude than in simulations without shear (see left panel of Figure 4)
- Radiative cooling enables groving of the cloud top and counteracts dilution due to wind shear (see Figures 5 and 6).
- Virtual aircraft method produces comparable statistics as the statistics made for the whole domain except for the span between the maximum and tne minimum values at the given altitude (see figure 7).

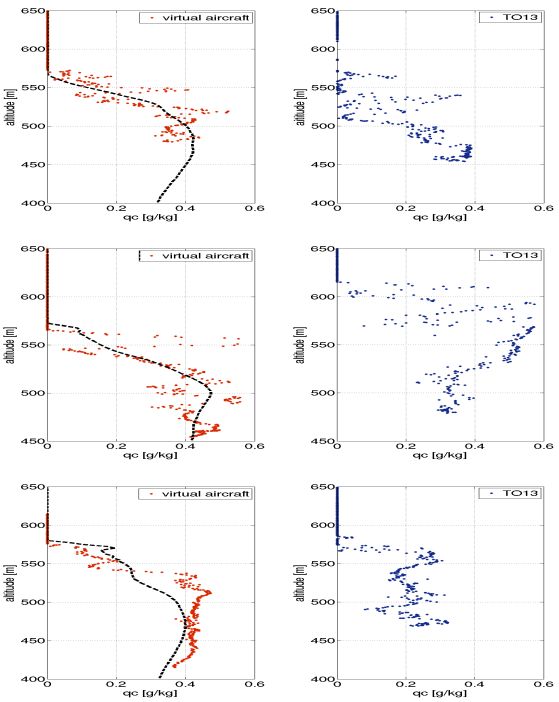

Figure 8: Comparison of examples of virtual aircraft data (left panels) with data from TO13 flight (right panels). Dashed black lines in left panels are single column profiles from a model.

- Profiles "collected" by the virtual aircraft look alike profiles from real airborne measurements. Fluctuations in the profiles result from the horizontal variability of the cloud.

References

Gerber, H., G. Frick, S. P. Malinowski, W. Kumala, and S. Krueger., 2013: Entrainment rates and microphysics in post stratocumulus. *J. Geophys. Res.-Atmos.*, **118**, 12,094–12,109, doi: 10.1002/jgrd.50878.

Gerber, H., S. P. Malinowski, A. Bucholtz, and T. Thorsen, 2014: Radiative cooling of stratocumulus. *14th Conf. on Atmospheric Radiation*, Boston, MA, Amer. Meteor. Soc., 9.3.

Kurowski, M. J., S. P. Malinowski, and W. W. Grabowski, 2009: A numerical investigation of entrainment and transport within a stratocumulus-topped boundary layer. *Quarterly Journal of the Royal Meteorological Society*, **135**, 77–92.

Malinowski, S. P., and Coauthors, 2013: Physics of stratocumulus top (post): turbulent mixing across capping inversion. *Atmospheric*

Chemistry and Physics, **13 (24)**, 12 171–12 186, doi:10.5194/acp-13-12171-2013, URL http://www.atmos-chem-phys.net/13/12171/2013/.

Piotrowski, Z. P., A. Wyszogrodzki, and P. K. Smolarkiewicz, 2011: Towards petascale simulation of atmospheric circulations with soundproof equations. *Acta Geophysica*, **59 (6)**, 1294–1311.

Prusa, J., P. Smolarkiewicz, and A. Wyszogrodzki, 2008: Eulag, a computational model for multiscale flows. *Comput. Fluids*, **37**, 1193–1207, doi:10.1016/j.compfluid.2007.12.001.

Stevens, B., and Coauthors, 2005: Evaluation of large-eddy simulations via observations of nocturnal marine stratocumulus. *Monthly Weather Review*, **133**, 1443–1462.